Photocyclic initiating system for free radical photopolymerization studied through holographic recording

Ahmad Ibrahim, Xavier Allonas, Christian Ley, Bandar El Fouhaili, Christiane Carré

Photocyclic initiating system for free radical photopolymerization studied through holographic recording

A. Ibrahim[a], X. Allonas[a], C. Ley[a], B. El Fouhaili[a], C. Carré[b]

[a]Department of Photochemistry, CNRS, University of Haute Alsace, ENSCMu, 3 rue Alfred Werner, 68093 Mulhouse Cedex – France.
[b]CNRS, UMR 6082 FOTON, Enssat, 6 rue de Kerampont, BP 80518, 22305 Lannion – France

This paper discusses the efficiency of photocyclic initiating system (PCIS) based on a pyrromethene dye (EMP), an amine as electron donor (NPG) and an iodonium salt as electron acceptor (I250) under homogenous irradiation and holographic recording. It is shown that the PCIS is more efficient than the corresponding two component systems. This high efficiency is due to a photocyclic reaction that takes places during the irradiation, inducing the recovery of the dye in the ground state and the formation of two initiating radicals. The beneficial effect on the rate of grating formation and on the diffraction efficiency is clearly noticed. At high irradiation time, the fast polymerization observed with EMP-NPG-I250 even induces the polymerization in the dark fringes leading to a decrease of the holographic diffraction efficiency. This confirms the high performance of the photoinitiating system which can be used in holographic recording provided that the irradiation dose could be controlled.

Keywords: Photoinitiating system, pyrromethene dye, laser spectroscopy, photopolymerization, holographic recording.

1. Introduction

Photopolymerizable systems usually contain a photoinitiator systems (PIS) and a monomer. To initiate photopolymerization reactions, the systems require photochemical reactions by photoinitiators which absorb light energy, from photons. They reach an excited state from which active centers such as free radicals that initiate the polymerization, are generated. Photoinitiator systems can be classified according to the number of components involved. Type I systems contain a single-component photoinitiator (unimolecular fragmentation mechanism), while type II systems are based on two components (bimolecular electron transfer or hydrogen abstraction mechanism) and finally three components initiator systems were developed to enhance the efficiency of type II systems [1,2].

Type I photoinitiator systems is extremely efficient systems because back electron transfer step does not occur and produce high rate of cleavage [2]. Another important advantage of type I is the short life time of the excited state [1,2]. One-component photoinitiator systems are only active for UV wavelength and UV light sources [2]. Two-component photoinitiator systems are more versatile initiators for both ultra violet (UV) curing systems and visible light induced systems because the choice of the light absorbing molecule (the photosensitizer) is not limited to UV absorbing molecule and can be selected in organic dyes. These PIS are relatively inexpensive although less efficient than type I PIS [2]. To improve and prevent the limitation of polymerization kinetics, three-component PIS were developed [3-8] and have been found to be by far more efficient than the corresponding two-component systems [9-11]. They generally include a photosensitizer which is typically a dye, an electron donor and as third component an electron acceptor [3-8].

In this work, the efficiency of a photoinitiating system based on a pyrromethene dye (EMP) was studied using a photopolymerizable resin optimized for holographic recording. Beside the dye, two different coinitiators were added, an amine (NPG) as electron donor and an iodonium salt (I250) as electron acceptor (Scheme 1). The behavior of the corresponding photoinitiating systems was investigated under homogenous irradiation (RT-FTIR) and holographic recording. The obtained grating formation is discussed according to the measured RT-FTIR photopolymerization kinetics. Moreover, the mechanisms of interaction between the

excited states of the dye and the coinitiators were identified using fluorescence spectroscopy and laser flash photolysis experiments.

2. Experimental

2.1. Materials

1, 3, 5, 7, 8 - pentamethyl - 2, 6 - diethyl -pyrromethene - difluoroborate complex (EMP) was purchased from Exciton. N-Phenylglycine (NPG) was obtained from Aldrich and (4-methylphenyl)[4-(2-methylpropyl)phenyl]-iodonium hexafluorophosphate (I250) was gifts from Ciba Spa. (Switzerland). Their chemical structures are given in Scheme 1. The photophysical and electrochemical properties of EMP and used coinitiators are given in Table 1.

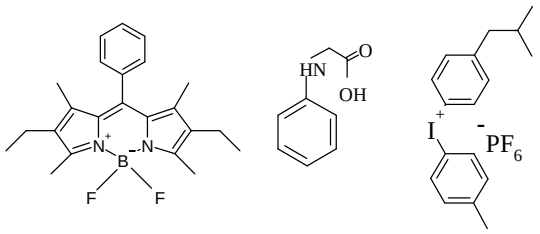

EMP **NPG** **I250**

Scheme 1.

Table 1. Photophysical and electrochemical properties of EMP, NPG and I250 (a) from reference [12] and b) from this work).

	EMP[a)]	NPG[b)]	I250[b)]
λ_{max} (nm)	515		
λ_{max}^{EM} (nm)	536		
ε_{max} (M^{-1} sec^{-1})	70400		
E_S *(kcal/mol)*	54.6		
τ_f (ns)	6.8		
φ_f	0.85		
E_T *(kcal/mol)*	40.2		
τ_T (µs)	33		
E_{ox} *(V/SCE)*	1.07	0.93	
E_{red} *(V/SCE)*	-1.24		-0.82

The reactive resin was a liquid mixture of 30 wt% of a hexafunctional aliphatic urethane acrylate oligomer (Ebecryl 1290), 15 wt% of 1,1,1,3,3,3-hexafluoroisopropyl acrylate, 15 wt% of vinyl neononanoate, 4.6 wt% of N-vinyl pyrrolidinone and 4.6 wt% of trimethylolpropane tris(3-mercaptopropionate) [7, 13-16]. Beside the Ebecryl 1290 purchased from Cytec, the other components of the resin mixture were purchased from Aldrich. For all experiments, the 0.2 wt% dye was introduced in the resin and the concentrations of coinitiators were fixed at 2.0 x 10^{-2} M and 1.75 x 10^{-2} M for NPG and I250 respectively.

2.2. RT-FTIR experiments

The photopolymerization kinetics were followed by real time FTIR spectroscopy (Vertex 70, Bruker) as described elsewhere [17-18]. Rates of polymerization Rp are easily calculated from the monomer conversion curves C(%) and from the initial acrylate double bond concentration [M_0] according to :

$$Rp = \frac{[M_0]}{100}\frac{dC(\%)}{dt} \qquad (1)$$

In the following the value $(Rp/[M]_0)x\ 100$ will be reported for the polymerization rates and noted by $R'p$ in the different tables. A diode laser emitting at 532 nm was used to irradiate the sample within the RT-FTIR chamber.

2.3 Holographic recording experiments

The samples were prepared by embedding the photopolymerizable formulation between two glass-substrates. Calibrated glass beads were used as spacers to guarantee the thickness of the system around 20 µm. During holographic recording, a sinusoidal light pattern is generated by the interferences of the two incident plane waves and is converted into a modulation of the refractive index in the photopolymerizable matrix [19-20]. The two incident s-polarized beams were of equal intensity, corresponding to a total power density of 25 mW/cm^2 on the photosensitive sample with a beam diameter of 2.5 cm and obtained with a 514 nm Coherent Innova 308C Argon Ion laser. The fringe spacing is adjusted to ca. 0.9 µm and exposure duration of ca. 90 s. The fact that no chemical post-treatment was needed for this recording medium, allowed the continuous follow up of the process during exposure with an inactinic reading light beam (HeNe laser at 633 nm) which is more or less diffracted. The diffraction efficiency at 633 nm (η) was defined by the ratio of the intensity of the first diffraction order to the diffracted plus transmitted light intensities. This measurement instead of the ratio of the diffracted intensity by the incident intensity at 633 nm was performed in order to rule out Fresnel losses in the determination of the grating diffraction efficiency. The rate of grating formation R_η is calculated as:

$$R_\eta = d\eta/dt \qquad (2)$$

2.4 Spectroscopy measurements

The nanosecond transient absorption setup is based on a Nd:Yag laser (Powerlite 9010, Continuum) operating at 10 Hz. This laser delivers nanosecond pulses at 532 nm with an energy about 5-8 mJ. The transient absorption analyzing system (LP900, Edinburgh Instruments) consists in a 450W pulsed xenon arc lamp, a Czerny–Turner monochromator, a fast photomultiplier and a transient digitizer.[21-22].

3. Pyrromethene dyes in three-component photoinitiating systems

The efficiency of pyrromethene dyes has been outlined in three-component systems based on photoinduced electron transfer process. Their use in photopolymerization experiments was highlighted in recent papers [5-7].

3.1. Photopolymerization experiments

The efficiency of different combinations of EMP, NPG and I250 as photoinitiating systems was evaluated using the RT-FTIR technique and holographic recording. Figure 1 (a) shows the kinetics of photopolymerization obtained for the different formulations under an intensity of 25 mW/cm^2 at 532 nm, and Table 2 collects the corresponding inhibition times t_{inh}, maximum rates of polymerization $R'p$ and final conversion C_{max}.

It is found that EMP alone is not able to perform the conversion of the resin. In the presence of NPG low photopolymerization efficiency was noticed with 37% conversion and 0.9 s^{-1} polymerization rate. While, holographic recording experiments show that this system does not have a sufficient efficiency to record a hologram, i.e. the diffraction efficiency value η is zero (Figure 1 (b), Table 2). This behavior could be related to the gelation point of the photopolymerized system [7], where this low conversion percentage obtained under homogenous irradiation indicates the formation of short polymeric chains unable to form any solid film but allow an increasing of the medium viscosity. As consequence, these chains are able to diffuse in the dark areas under holographic recording inducing a vanishing of the modulation of the refractive index.

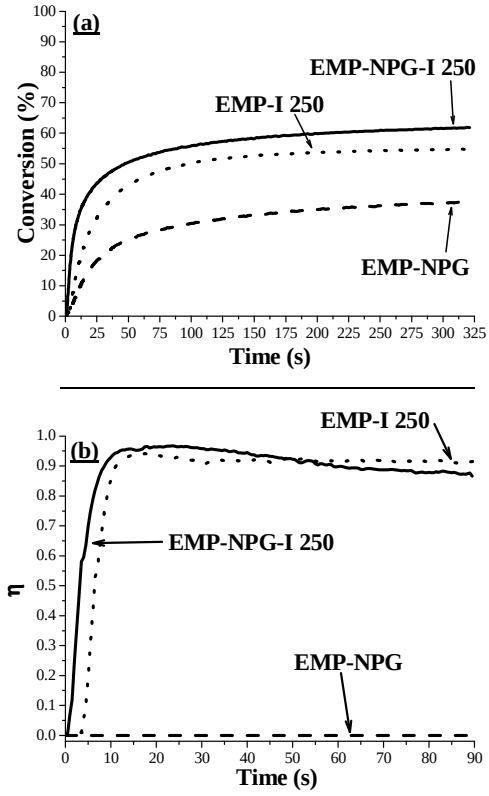

Figure 1. (a) Conversion curves of the EMP-NPG-I 250 photoinitiating systems upon green laser exposure at 532 nm (irradiance = 25 mW/cm²); (b) Variation of the diffraction efficiency of the different photoinitiating systems as a function of time for an irradiance of 25 mW/cm^2 at 514 nm.

Table 2. Characteristic parameters for the EMP-NPG-I 250 photoinitiating systems. Inhibition times t_{inh}, maximum rates of polymerization $R'p$ (s^{-1}), final conversion C_{max} (%), maximum diffraction efficiency (η_{max}) and maximum grating of formation R_η(s^{-1}).

Parameters	**NPG**	**I250**	**NPG-I250**
t_{inh} (s)[a]	1.8	2.1	0.8
R'_p [a] (s^{-1})	0.9	2.3	6.3
C_{max}(%)[a]	37.5	54.4	61.8
η_{max} [b]	0	0.94	0.98 (0.85)[c]
R_η(s^{-1})[b]	0	0.21	0.25

a) Results obtained for homogeneous irradiation at 532 nm, 25 mW/cm². b) Results obtained for inhomogeneous irradiation at 514 nm using holography setup, 25 mW/cm². c) The value in brackets corresponds to the final diffraction efficiency.

Moreover, the second two-component PIS based on EMP-I250 appears to be more efficient with 54% final conversion and 2.3 s^{-1} maximum polymerization rate. In addition this system leads to the formation of a diffraction grating with a maximum rate of grating formation of about 0.21 s^{-1} and a maximum diffraction efficiency η around 94%.

As can be seen, the addition of electron donor NPG to the EMP-I250 system makes the photopolymerization kinetic more efficient. The conversion percentage increase noticeably to reach 62% but the rate of polymerization reached 6.3 s^{-1} nearly 3 times faster than the EMP-I250 PIS. Notably this system leads to maximum diffraction efficiency close to unity with higher maximum grating of formation around 0.25 s^{-1}. If the grating formation rate of EMP-I250-NPG is close to the EMP-I250 PIS, the inhibition grating formation time is significantly lower in the 3 components PIS (see figure 1), outlining the most efficient radical

generation.

The limited conversion percentage obtained for the EMP-NPG-I250 (close to that obtained with the two component system EMP-I250) result from the fast solidification of the medium that occurs before full conversion under homogenous irradiation [23-24]. But, a different behavior take places under holographic recording where the fast solidification of the exposed regions lead to the formation of a gradient in the monomer concentration between the exposed and the exposed zones. This leads to a driving force which promotes the diffusion of the monomer from the unexposed regions to the exposed ones [25-27]. Moreover, the diffraction efficiency behavior of the three component photoinitiating system is different comparing to the corresponding two component systems. A slight decrease of the diffraction efficiency was observed after the fast building up of the grating to reach a value of about 85% after 90 seconds of irradiation. According to the literature, this decrease could result from the polymerization in the dark fringes due to the high efficiency of the three component photoinitiating system [7].

These results show clearly that the three component photoinitiating systems are more efficient than their corresponding two component systems. In some conditions, this difference in efficiency does not appear clearly under homogenous irradiation. But the use of holographic recording outlines the differences in photoinitiating systems reactivity.

3.2. Mechanism of interaction

According to the literature, a photoinduced electron transfer process take places between the singlet excited state of the EMP and the coinitiators [5-7]. The values of the Gibbs free energy values (ΔG_{et}) for the photoinduced electron transfer were calculated according to the Rhem-Weller equation [28] as follows:

$$\Delta G_{et} = E_{ox} - E_{red} - E^{*} + C \qquad (4)$$

where E_{ox} and E_{red} are the half-wave oxidation and reduction potentials for the donor and the acceptor, respectively. E* stands for the energy of the excited state. The Coulombic term C is usually neglected in polar solvent. The calculated ΔG_{et} values are gathered in Table 3. As can be seen, the intermolecular electron transfer process is not favourable in the ground state, a fact which rules out any dark reaction. Moreover, endergonic ΔG_{et} are obtained for the reaction of the triplet excited state of EMP (^{3}EMP) and all coinitiators, indicating that the photoinduced electron transfer process is not thermodynamically favourable from ^{3}EMP. The calculated values for the intermolecular singlet electron transfer reactions are favorable, indicating that the dye can be reduced in the presence of the electron donor NPG or oxidized with I250. Moreover, as EMP exhibits a high fluorescence quantum yield (φ_f =0.85) [12], its photoreactivity is expected to occur predominately from the singlet excited state ^{1}EMP. In addition, the calculated ΔG_{et} for the reaction ^{1}EMP with I250 is two times more exergnonic than the one calculated with NPG indicating that ^{1}EMP should reacts predominately with I250 first in the case of the three component system.

Table 3. Gibbs free energy (ΔG_{et}) values for ground and excited states electron transfer reactions of EMP/coinitiator systems.

ΔG_{et} (eV)	Ground state	Singlet state	Triplet state
NPG	2.17	-0.2	0.43
I250	1.89	-0.48	0.15

In order to get more insights into the photochemical process that take place during the photopolymerization process and to explain the high reactivity of the three component system, the interactions between the excited states of the pyrromethene dye and the coinitiators were investigated using different spectroscopy experiments.

Figure 2 shows the fluorescence spectrum of EMP in acetonitrile in the presence of increasing amounts of I250. The corresponding rate constant of quenching k_q can be calculated from the decrease of the fluorescence intensity by using the Stern-Volmer equation.

$$I_0/I = 1 + k_q \tau_0 [Q] \qquad (3)$$

where I_0 and I are the fluorescence intensities in the absence and in the presence of quencher Q, respectively, and τ_0 is the fluorescence lifetime of EMP (6.8 ns [12]). As shown in Table 4, the singlet quenching rate constants obtained for I250 is 10 times higher than that measured with NPG in line with calculated ΔG_{et} (vide

supra). These constants are also in line with the photopolymerization experiments under homogenous irradiation and holographic recording where the system based on I250 showed greater results compared to the one based on NPG.

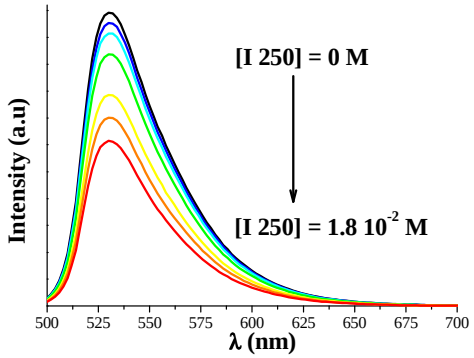

Figure 2. Fluoresence spectrum of EMP in acetonitrile quenched by the addition of I250 under Ar bubbling (Excitation at 494 nm).

Pseudo first order reaction rates (i.e; k_q x [coinitiators]) were calculated at initiator concentrations used in the resin formulation, namely [NPG] = 2.0 x 10^{-2} M and [I 250] = 1.75 x 10^{-2} M (Table 4). As can be seen, the NPG reaction rate is 10 times lower than I250. These data indicate that the ^{1}EMP reacts first with I250 in the case of the three component system.

Table 4. ^{1}EMP quenching rate constants k_q and corresponding pseudo-first order reaction rates with the different coinitiators studied.

Coinitiator	k_q (M^{-1} s^{-1})	k_q x [Coinitiator] (s^{-1})
NPG	8.5 10^8	1.7 10^7
I250	9.0 10^9	1.6 10^8

To confirm the regeneration of EMP, the photobleaching signal of EMP was studied by laser flash photolysis. The photobleaching signal observed at 510 nm after addition of I250 and after laser pulse excitation at 532 nm is presented in Figure 3. As can be seen, the addition of I250 to the EMP solution leads to the bleaching of the dye, as a consequence of the formation of the dye radical cation EMP•+ which do not recombine in the time window of the experiment. Due to their low absorption properties, EMP•+ cannot be detected [12, 29]. After the addition of increasing amount of NPG to the EMP/I250 solution, a decrease of the photobleaching of EMP is observed (see Figure 3) indicating that a recovery of the dye occurs.

This recovery of EMP ground state is be the result of the reduction reaction of EMP•+ by NPG. Indeed, if one assumes that the reduction potential of EMP•+ is +1.07 V/SCE, a ΔGet of -0.14 eV for the electron transfer reaction between NPG and EMP•+ is calculated, indicating that this reaction is thermodynamically favorable. The radical cation NPG•+ created during this reaction undergoes a deprotonation reaction, which yields the formation of a second initiating radical.

According to these data, the proposed mechanism for EMP-NPG-I250 exhibits a photocyclic behavior, as exemplified Scheme 2.

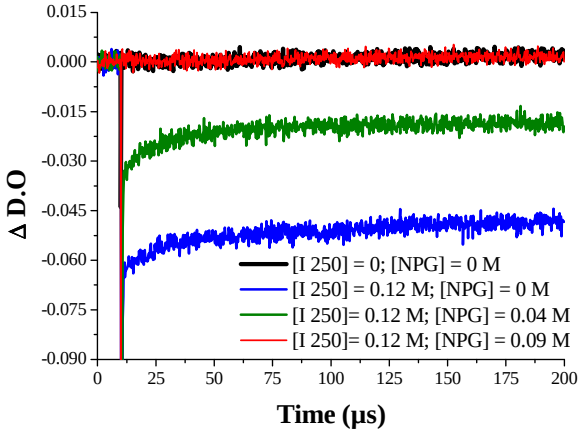

Figure 3. EMP photobleaching signal measured at 510 nm in acetonitrile solution under Ar bubling: effect of NPG addition on EMP-I250 solution (Excitation at 532 nm).

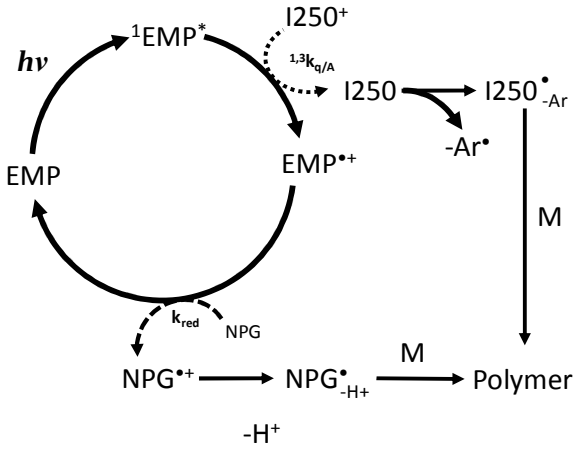

Scheme 2.

4. Conclusion

In this paper, the efficiency of a photoinitiating system based on EMP-NPG-I250 was examined using an optimized resin mixture for holographic recording. RT-FTIR photopolymerization kinetics show that the three component system is more efficient compared to the corresponding two component photoinitiating systems. Diffraction efficiency close to the unity was obtained for this system. Holographic recording experiments allowed better identification of the differences between the PIS that are not detected with conventional RT-FTIR. The photocyclic reaction resulted from beneficial side reaction between the amine and the formed radical cation of dye explains the high efficiency observed for the three component photoinitiating system. This reaction decreases the photobleaching of the dye and leads to the formation of more initiating radicals.

References

1. X. Allonas, C. Croutxe-Barghorn, J.P. Fouassier, J. Lalevée, J.P. Malval, F. Morlet-Savary, "Laser in the photopolymer area," in *Lasers in Chemistry*, Vol II, M. Lackner, Ed. Weinheim, 2008, pp. 1001-1027.
2. A. Ibrahim, L. Di Stefano, O. Tarzi, H. Tar, C. Ley, X. Allonas, *Photochem. Photobiol.* **89** (2013) 1283.
3. X. Allonas, J.P. Fouassier, M. Kaji, M. Miyasaka, T. Hidaka, *Polymer*, **42** (2001) 7627.
4. X. Allonas, J. P. Fouassier, M. Kaji, Y. Murakami, *Photochem. Photobiol. Sci.*, **2** (2003) 224.
5. O. I. Tarzi, X. Allonas, C. Ley and J. P. Fouassier, *J. Polym. Sci. Polym. Chem.*, **48** (2010) 2594.

6. A. Ibrahim, C. Ley, O. I. Tarzi, J. P. Fouassier and X. Allonas, *J. Photopolym. Sci. Technol.*, **23** (2010) 101.
7. A. Ibrahim, C. Ley, X. Allonas, O. I. Tarzi, A. Chan Yong, C. Carre and R. Chevallier, *Photochem. Photobiol. Sci.*, **11** (2012) 1682.
8. H. Salmi, H. Tar, A. Ibrahim, C. Ley and X. Allonas, *Eur. Polym. J.*, **49** (2013) 2275.
9. Y. Bi and D. C. Neckers, *J. Photochem. Photobiol. Chem*, **74** (1993) 221.
10. D. F. Eaton, *Top. Cur. Chem.*, **156** (1990) 199.
11.T. Urano, E. Hino, H. Ito, M. Shimizu and T. Yamaoka, *Polymers for Advanced Technology*, **9** (1998) 825.
12. S. Suzuki, X. Allonas, J.-P. Fouassier, T. Urano, S. Takahara and T. Yamaoka, *J. Photochem. Photobiol. Chem.*, **181** (2006) 60.
13. M. De Sarkar, J. Qi and G. P. Crawford, *Polymer*, **43** (2002) 7335.
14. M. D. Schulte, S. J. Clarson, L. V. Natarajan, D. W. Tomlin and T. J. Bunning, *Liq. Cryst.*, **27** (2000) 467.
15. T. M. Roper, T. Kwee, T. Y. Lee, C. A. Guymon, C. E. Hoyle, *Polymer*, **45** (2004) 2921.
16. C. Carre, R. Chevallier, B. Mailhot, A. Rivaton, "*Basics and applications of photopolymerization reactions*, vol. 3", J.P. Fouassier, X. Allonas, Eds.; Research Signpost: Trivandrum, India, (2010) 175-84.
17. C. Decker, K. Moussa, *Macromolecules*, **22** (1989) 4455.
18. X. Allonas, C. Grotzinger, J. Lalevee, J.P. Fouassier, M. Visconti, *Eur. Polym. J.*, **37** (2001) 897.
19. S. Massenot, J.L. Kaiser, R. Chevallier, Y. Renotte, *Appl. Opt.*, 43 (2004) 5489.
20. S. Gallego, M. Ortuno, C. Neipp, C. Garcia, A. Beléndez, I. Pascual, *Opt. Com.*, 215 (2003) 263.
21. X. Allonas, J.P. Fouassier, L. Angiolini, D. Caretti, *Helv. Chim. Acta*, 84 (2001) 2577.
22. C. Dietlin, X. Allonas, A. Defoin, J. P. Fouassier, *Photochem. Photobiol. Sci.*, **7** (2008) 558.
23. C. Decker, *Prog. Polym. Sci.*, **21** (1996) 593.
24. C. Decker, *Macromol. Rapid Commun.*, **23** (2002) 1067.
25. J.R. Lawrence, F.T. O'Neill, J.T. Sheridan, *Optik*, **112** (2001) 449.
26. M.R. Gleeson, J. T. Sheridan, *J. Opt. Pur. Appl. Opt.*, **11** (2009) 024008.
27. M. Květoň, A. Havránek, P. Fiala, I. Richter, *Polym. Bull.*, **58** (2007) 253.
28. D. Rehm, A. Weller, *Isr. J. Chem.*, **8** (1970) 259.
29. G. Jones, S. Kumar, O. Klueva, D. Pacheco, *J. Phys. Chem. A*, **107** (2003) 8429.